



Disturbances in system dynamics of Ca^{2+} and IP_3 perturbing insulin secretion in a pancreatic β -cell due to type-2 diabetes

Vaishali¹ · Neeru Adlakha¹

Received: 27 February 2023 / Accepted: 27 April 2023 / Published online: 7 July 2023
© The Author(s), under exclusive licence to Springer Science+Business Media, LLC, part of Springer Nature 2023

Abstract

The individual study of Ca^{2+} and IP_3 dynamics respectively in a β -cell has yielded limited information about the cell functions. But the systems biology approaches for such studies have received very little attention by the research workers in the past. In the present work, a system-dynamics model for the interdependent Ca^{2+} and IP_3 signaling that controls insulin secretion in a β -cell has been suggested. A two-way feedback system of Ca^{2+} and IP_3 has been considered and one-way feedback between Ca^{2+} and insulin has been implemented in the model. The finite element method along with the Crank-Nicolson method have been applied for simulation. Numerical results have been used to analyze the impact of perturbations in Ca^{2+} and IP_3 dynamics on insulin secretion for normal and Type-2 diabetic conditions. The results reveal that Type-2 diabetes comes from abnormalities in insulin secretion caused by the perturbation in buffers and pumps (SERCA and PMCA).

Keywords System dynamics · Ca^{2+} · IP_3 · Insulin · Type-2 diabetes · FEM · Crank-Nicolson method

Introduction

Physiological functions like release of hormone and neurotransmitter, permeability of ionic channels, activity of enzymes, gene transcription, reproduction and apoptosis are all controlled by changes in cytosolic Ca^{2+} ions. The cytosolic concentration of Ca^{2+} ions in almost every cell type exhibits complex spatiotemporal dynamics. Ca^{2+} signals in a β -cell initiate the formation and secretion of insulin hormone, which is released when plasma glucose levels are high. Blood glucose levels in healthy adults must be kept within a tight range: typically 4–5 mM and usually, it lies between 3.5–7.0 mM in fasting subjects (Buchwald 2011). The increased glucose level can induce both types of diabetes mellitus, Type-1 and Type-2. The abnormalities in the β -cell functions are the primary reason for this elevation. It is a life-threatening metabolic disorder that affects 5–10% of

the people in developed countries (Rorsman et al. 2012). It is also generally understood that diabetes is complex with environmental factors such as excessive intake of calories and lack of physical movements, both of which contribute to obesity, increasing the chance of developing the disease (Boob-Bavnbek et al. 2008).

In pancreatic β -cells, the intracellular Ca^{2+} is the immediate controller of production and the secretion of insulin by exocytosis. The intracellular Ca^{2+} ions level is elevated by the influx of Ca^{2+} ions via voltage gated Ca^{2+} channel (VGCC) and various other components such as the source, pump, leak and so on. All these contribute to calcium control within the cell. Several experimental studies provide insights on the involvement of IP_3 in the functioning of IP_3R . Ca^{2+} signaling triggered by IP_3 is recognised to be crucial for normal cell functions and metabolic activities (Decrock et al. 2013). IP_3R are essential for various Ca^{2+} responses such as oscillations and waves inside the cell and hence crucial part in different models of Ca^{2+} regulations. The IP_3 releases ER Ca^{2+} by binding to the IP_3R . It is also crucial to remember that the IP_3 and Ca^{2+} pathway changes with age and these changes could have an impact in the development of diabetes. The expression of IP_3R which produces IP_3 was found to be lower in diabetic patients. Gallbladder emptying and gallstone development decrease as a result

✉ Vaishali
d20ma002@amhd.svni.ac.in
Neeru Adlakha
nad@amhd.svni.ac.in

¹ Department of Mathematics and Humanities, SVNIT,
Surat 395007, Gujarat, India

of the drop in the IP_3/Ca^{2+} signaling pathway which is a comorbidity typically linked with diabetes (Berridge 2016).

Numerous research workers conducted experimental inquiries with fruitful alternatives (Misler et al. 1992; Pertusa et al. 1999; Braun et al. 2008). During the last few decades, certain theoretical studies have also been conducted (Dupont and Erneux 1997; Rorsman 2005; Boob-Bavnbek et al. 2008; Rorsman et al. 2012; Rorsman and Braun 2013; Idevall-Hagren and Tengholm 2020). Crank in 1979 discussed the diffusion mechanism and techniques of their numerical solution in different media. In 1995, Bootman and Berridge highlighted the role of various channels in influx and efflux of Ca^{2+} ions for calcium signaling events in different tissues. Smith (1996a, 1996b) investigated the impact of rapid stationary as well as mobile buffers on calcium dynamics near an open Ca^{2+} channel by obtaining the analytical steady state solution.

Apart from these studies, excitable cells have been a keen interest of researchers for many years. Several studies have been performed to know the signaling patterns of these cells. Wagner et al. (2004) investigated $[Ca^{2+}]$ and IP_3 bistability in oocytes which is accomplished through calcium-feedback upon calcium-dependent IP_3 production and release of calcium mediated by IP_3 . Naik and Pardasani (2014, 2019) developed the mathematical models of spatio-temporal calcium variations in oocytes by incorporating the ryanodine receptor, VGCC, SERCA pump and diffusion coefficient. Role of Na^+/Ca^{2+} exchanger and calcium advection phenomenon in oocytes has been analyzed by Panday and Pardasani (2013, 2013). Tewari and Pardasani (2010, 2011a, 2011b) developed the mathematical models for neurons to investigate the impact of Na^+ influx and buffers on $[Ca^{2+}]$ profile. A mathematical model to explore the effect of buffers on the calcium profile of dendritic spines has been investigated by Tripathi et al. (2014, 2013). They also analyzed the calcium dynamics in neurons by incorporating J_{Leak} , J_{SERCA} and J_{RyR} along with the calcium diffusion coefficient as well as exogenous buffers like BAPTA and EGTA. Pathak and Adlakha (2015, 2016) constructed a mathematical model to analyze the calcium profile of myocytes by incorporating calcium diffusion, excess buffers, pump and leak for one dimensional spatio temporal case. Jha et al. (2016, 2013) constructed few mathematical models to explore the relationships among the parameters impacting Ca^{2+} dynamics such as source influx and diffusion coefficient in astrocytes by using finite volume and finite element method. Naik and Zu (2020) studied the spatiotemporal calcium profile of T-lymphocytes by framing the reaction-diffusion model. They solved their model by combining the finite element and finite difference methods. Hemant and Adlakha (2022) used the RBF approach and Runge-Kutta method to analyze the calcium reaction-diffusion model that includes the Ryanodine

receptor, SERCA pump, source amplitude and buffers for T-lymphocytes.

Pancreatic β -cells were among the first cell types to have the relationship of membrane oscillators and cytosolic Ca^{2+} dynamics studied in depth (Chay and Keizer 1983; Rinzel and Lee 1987). Magnus and Keizer (1997) devised a minimal mathematical model for describing the mitochondrial calcium management of pancreatic β -cells. Gopel et al. (1999) investigated the potassium current (K_{slow}) depending upon Ca^{2+} that gradually increases with respect to simulated islet burst in mouse pancreatic β -cells. Alteration in potassium current may help to terminate the bursting phenomenon depending upon Ca^{2+} , which promote the Ca^{2+} influx and secretion of insulin in a β -cell. Goforth et al. (2002) studied that how disrupting $[Ca^{2+}]$ by inhibiting Ca^{2+} absorption into the ER by two different agents claimed to impede the SERCA, thapsigargin (1–5 μM) or insulin (200 nM) inhibit the calcium-dependent potassium current. Fridlyand et al. (2010) constructed a mathematical model by involving the pacemaker candidates of bursts action as well as cytoplasmic Ca^{2+} oscillations in a β -cell. They also formulated a precise mathematical model of β -cell ionic fluxes by incorporating the major pumps and channels of plasma membrane 2003 and showed that changes in Ca^{2+} concentration can modulate inositol lipid-specific phospholipase activity which in turn can stimulate IP_3 -production in the β -cell. Varadi et al. (1995) in their work investigate the PMCA and SERCA are associated in dynamic Ca^{2+} transport in a β -cell lines (RINm5F, T15, HIT, MIN6) and islets. Berridge (2016) explained theoretically how the major Ca^{2+} route controls processes like muscles contraction, formation of memory in neurons and secretion of insulin and described how IP_3/Ca^{2+} signaling pathways are engaged in a number of biological processes. Sabatini et al. (2019) in their work briefly highlighted the classical pathways of calcium regulation in β -cells and as well as how they monitor the Ca^{2+} mobility in several microdomains and organelles. The significance of Ca^{2+} signaling in β -cell has been discussed by Klec et al. (2019). They provide the role of alterations in β -cell Ca^{2+} signaling and its importance in the development of diabetes.

The study of calcium signaling in various cells individually without the feedback of other signaling systems yielded limited information. Thus, from the last few years coupled dynamics have been proven a powerful tool to investigate the signaling pattern for different cells using mathematical models 2003, 2022a, 2022b, 2022c, 2022d, 2023, 2019a, 2019b, 2004. Recently, a dynamic interaction between glucose, insulin, ATP and calcium in β -cell has been presented by Das et al. (2020) with the help of delay differential equations. Paul et al. (2022) performed a study to analyze the glucose-stimulated insulin secretion process through a

six-dimensional model by incorporating calcium and ATP and highlight the responsible factors in the progression of diabetes in insulin resistance conditions in β -cell. There are several research papers describing the relationship between the Ca^{2+} and IP_3 (De Young and Keizer 1992; Dupont and Erneux 1997; Smith 1996a; Sneyd et al. 1995; Sneyd and Falcke 2005). The β -cell models reported in the literature focused only on temporal dynamics but due to the movement of signaling ions inside the cytosol the diffusion process also takes place. As far as we are aware no model is reported for interdependent spatiotemporal Ca^{2+} and IP_3 dynamics in a β -cell. Further, no study is reported for impacts of perturbation in Ca^{2+} and IP_3 dynamics on insulin secretion in a β -cell. The primary goal of the present work is to establish a mathematical model of interdependent spatiotemporal Ca^{2+} and IP_3 homeostasis in a β -cell to gain a better understanding of this complex regulatory network. A two-way feedback of Ca^{2+} and IP_3 dynamics in a β -cell is incorporated in the model. The processes like SERCA pump, leak, IP_3R , VGCC and PMCA are employed in the proposed model. Numerical simulations are performed using the finite element and the Crank-Nicolson method. With the use of numerical findings, it has been determined how changes in Ca^{2+} and IP_3 dynamics affect the secretion of insulin in both normal and Type-2 diabetes conditions.

Mathematical model

The equations for cytoplasmic $[Ca^{2+}]$ and $[IP_3]$ handling for the β -cell can be written as Fridlyand et al. (2003); Higgins et al. (2006); Jha et al. (2013); Wagner et al. (2004):

$$\begin{aligned} \frac{\partial [Ca^{2+}]}{\partial t} = & D_{Ca} \nabla^2 [Ca^{2+}] \\ & - k_i^+ [B_i]_{\infty} ([Ca^{2+}] - [Ca^{2+}]_{\infty}) \\ & + \frac{J_{leak} - J_{SERCA} + J_{IP_3R}}{F_c} \\ & - J_{pump} + J_{VGCC}, \end{aligned} \tag{1}$$

$$\begin{aligned} \frac{\partial [IP_3]}{\partial t} = & D_{IP_3} \nabla^2 [IP_3] \\ & + \frac{J_{production} - \lambda(J_{kinase} + J_{phosphate})}{F_c}. \end{aligned} \tag{2}$$

In Eq. 1 the first term on the right is diffusion term and second term is the reaction term. The symbols used in above equations are defined in Table 1.

$$J_{leak} = P_{ER}([Ca^{2+}]_{ER} - [Ca^{2+}]), \tag{3}$$

$$J_{SERCA} = \frac{P_{SERCA}^{max} [Ca^{2+}]^2}{k_{pump}^2 + [Ca^{2+}]^2}, \tag{4}$$

$$J_{IP_3R} = P_{IP_3R} m^3 h^3 ([Ca^{2+}]_{ER} - [Ca^{2+}]). \tag{5}$$

According to Li and Rinzel (1994) model:

$$m = \frac{[IP_3]}{[IP_3] + K_{IP_3}} \frac{[Ca^{2+}]}{[Ca^{2+}] + K_{Act}}. \tag{6}$$

The variable h denotes the percentage of subunits that haven't been inactivated by Ca^{2+} (Keizer and Magnus 1989; Wagner et al. 2004):

$$\frac{dh}{dt} = \frac{h_{\infty} - h}{\tau}, \tag{7}$$

where τ is the inactivation time scale. h_{∞} denotes the equilibrium value and defined as follows:

$$h_{\infty} = \frac{K_{Inh}}{K_{Inh} + [Ca^{2+}]}, \tag{8}$$

$$J_{pump} = \frac{P_{mCa} [Ca^{2+}]^2}{k_{pCa}^2 + [Ca^{2+}]^2}, \tag{9}$$

$$J_{VGCC} = \frac{-I_{Ca}}{Z_{Ca} F V_c}, \tag{10}$$

where Jha et al. (2013),

$$I_{Ca} = P_{Ca} Z_{Ca}^2 \frac{F^2 V_p}{RT} \frac{[Ca^{2+}] - [Ca^{2+}]_{\infty} \exp(-Z_{Ca} \frac{F V_p}{RT})}{1 - \exp(-Z_{Ca} \frac{F V_p}{RT})}. \tag{11}$$

The Ca^{2+} -induced IP_3 production is given by Wagner et al. (2004):

$$J_{production} = P_{production} \frac{[Ca^{2+}]^2}{k_{production}^2 + [Ca^{2+}]^2}. \tag{12}$$

The IP_3 degradation in Eq. 2 is given by $\lambda(J_{kinase} + J_{phosphate})$. The J_{kinase} and $J_{phosphate}$ denotes the kinase flux and phosphate flux respectively and defined as Wagner et al. (2004):

$$J_{kinase} = (1 - \theta) V_1 \frac{[IP_3]}{2.5 + [IP_3]} + \theta V_2 \frac{[IP_3]}{0.5 + [IP_3]}, \tag{13}$$

$$J_{phosphate} = V_3 \frac{[IP_3]}{(30 + [IP_3])}, \tag{14}$$

$$\theta = \frac{[Ca^{2+}]}{(0.39 + [Ca^{2+}])}. \tag{15}$$

Table 1 Biophysical parameters and numerical data

Notation	Name of the parameter	Numerical value
D_{Ca}	Diffusion coefficient for calcium	$200 \mu m^2 sec^{-1}$ Jha et al. (2013)
D_{IP_3}	Diffusion coefficient for IP_3	$283 \mu m^2 sec^{-1}$ Wagner et al. (2004)
k_i^+	Association rate of EGTA	$1.5 \mu M^{-1} sec^{-1}$ Smith et al. (1996b)
	Association rate of BAPTA	$600 \mu M^{-1} sec^{-1}$ Smith et al. (1996b)
$[B_i]_\infty$	EGTA Buffer	$15 \mu M$ (Assumed)
	BAPTA Buffer	$0.04 \mu M$ (Assumed)
$[Ca^{2+}]_\infty$	Intracellular free Ca^{2+} concentration at rest	$0.1 \mu M$ Pertusa et al. (1999)
F_c	Fraction of cytosolic and total cell volume	0.83 Wagner et al. (2004)
F_e	Fraction of ER and total cell volume	0.17 Wagner et al. (2004)
F	Faraday's constant	$96487 \text{ Coulombs Mole}^{-1}$ Panday and Pardasani (2013)
V_c	Volume of cytosol	$5.84 \times 10^{-11} \mu m^3$ Panday and Pardasani (2013)
λ	Scaling factor of production rate of IP_3	30 Wagner et al. (2004)
P_{ER}	Leak permeability of Ca^{2+} from ER	$0.1 sec^{-1}$ Fridlyand et al. (2003)
$[Ca^{2+}]_{ER}$	Concentration of Ca^{2+} in ER	$22.8 \mu M$ Fridlyand et al. (2003)
P_{SERCA}^{max}	Maximum pumping rate of SERCA	$0.65 \mu M sec^{-1}$ Wagner et al. (2004)
K_{pump}	Half-maximum pump activity of SERCA	$0.4 \mu M$ Wagner et al. (2004)
P_{IP_3R}	Rate constant of IP_3 receptor	$8.5 sec^{-1}$ Wagner et al. (2004)
K_{IP_3}	Dissociation constant of activating IP_3 binding site	$0.15 \mu M$ Wagner et al. (2004)
K_{Act}	Dissociation constant of activating Ca^{2+} binding site	$0.8 \mu M$ Wagner et al. (2004)
K_{Inh}	Dissociation constant of inhibiting Ca^{2+} binding site	$1.9 \mu M$ Wagner et al. (2004)
$P_{production}$	Maximum rate of IP_3 production	$0.075 \mu M sec^{-1}$ Wagner et al. (2004)
$K_{production}$	Michaelis constant for Ca^{2+} activation	$0.4 \mu M$ Wagner et al. (2004)
τ	Inhibition time constant	$2 sec$ Wagner et al. (2004)
P_{mCa}	Maximum pumping rate of PMCA	$28 \mu M sec^{-1}$ Higgins et al. (2006)
k_{pCa}	Half-maximum pump activity of PMCA	$0.425 \mu M$ Higgins et al. (2006)
V_1	Maximum rate constant at low Ca^{2+} (3-kinase)	$0.001 \mu M sec^{-1}$ Wagner et al. (2004)
V_2	Maximum rate constant at high Ca^{2+} (3-kinase)	$0.005 \mu M sec^{-1}$ Wagner et al. (2004)
V_3	Maximum rate constant (phosphatase)	$0.02 \mu M sec^{-1}$ Wagner et al. (2004)
Z_{Ca}	Valency of Ca^{2+}	2 Panday and Pardasani (2013)
$[Ca^{2+}]_0$	Extracellular Ca^{2+} Concentration	$3 mM$ Panday and Pardasani (2013)
V_p	Membrane Potential	$-0.03 V$ Panday and Pardasani (2013)
R	Gas Constant	$8.314 \text{ Joule/Kelvin Mole}$ Panday and Pardasani (2013)
T	Absolute Temperature	$300 K$ Panday and Pardasani (2013)
Ca_{null}	Minimal Ca^{2+} necessary for insulin release	$0.1 \mu M$ Pedersen et al. (2005)
I_{slope}	Measure of Ca^{2+} sensitivity of secretion	210 Pedersen et al. (2005)
τ_a	Time constant	$10 sec$ Pedersen et al. (2005)
σ_{Ca}	Source influx	$20 pA$ (Assumed)

The $[Ca^{2+}]_{ER}$ can be eliminated as:

$$[Ca^{2+}]_T = F_c[Ca^{2+}] + F_e[Ca^{2+}]_{ER}. \quad (16)$$

Initial and boundary conditions

The flux boundary condition for the source is provided by, where it is considered that the calcium source is present at

$x=0 \mu m$ (Smith et al. 1995):

$$\lim_{x \rightarrow 0} \left(-D_{Ca} \frac{\partial [Ca^{2+}]}{\partial x} \right) = \sigma_{Ca}. \quad (17)$$

The other end of the boundary is maintained at background concentration and expressed as given below:

$$\lim_{x \rightarrow 10} [Ca^{2+}] = 0.1 \mu M. \quad (18)$$

The boundary conditions for IP_3 are defined (Wagner et al. 2004):

$$\lim_{x \rightarrow 10} [IP_3] = 0.16 \mu M, \quad (19)$$

$$\lim_{x \rightarrow 0} [IP_3] = 3 \mu M. \quad (20)$$

At initial time $t=0$ msec the system is supposed to be at rest and thus the initial calcium concentration at rest is given by:

$$\lim_{t \rightarrow 0} [Ca^{2+}] = 0.1 \mu M, \quad (21)$$

$$\lim_{t \rightarrow 0} [IP_3] = 0.16 \mu M. \quad (22)$$

Insulin secretion

The influx of Ca^{2+} through different channels result in increased cytosolic calcium and exocytosis of insulin granules. It is assumed that any stimulation that causes a Ca^{2+} influx into the β -cell will cause the release of insulin. But, there are some Ca^{2+} chelators (like EGTA and BAPTA), which suppress the insulin secretion (Idevall-Hagren and Tengholm 2020; Pertusa et al. 1999). The rate at which a β -cell secrete insulin is given as follows (Pedersen et al. 2005):

$$\frac{d[I]}{dt} = \frac{I_{\infty}(Ca) - [I]}{\tau_a}, \quad (23)$$

where $I_{\infty}(Ca)$ denotes equilibrium secretion rate and is defined as:

$$I_{\infty}(Ca) = \begin{cases} I_{slope}([Ca^{2+}] - C_{anull}) & \text{for } [Ca^{2+}] \geq C_{anull} \\ 0 & \text{for } [Ca^{2+}] < C_{anull} \end{cases},$$

where I_{slope} measures the Ca^{2+} sensitivity of secretion (see Table 1) and C_{anull} represents the minimal Ca^{2+} concentration necessary for insulin release.

The numerical solution of the model given by the Eqs. 1–22 was obtained using the finite element approach. The finite element procedure used here is given in the Appendix. Taylor series expansion is applied for handling the non-linear terms present in the model. The cell is discretized into 40 elements and piecewise linear shape function is used for interpolation. The time derivatives have been handled using the Crank-Nicolson method which has been simulated using MATLAB to produce numerical results. After obtaining the numerical solution of the model given by the Eqs. 1–22 by finite element method along spatial dimension and then the Crank-Nicolson method is employed along temporal dimension to solve the Eqs. 1–23. The numerical data of various parameters employed for simulation is given in the Table 1.

Table

Results and discussion

The results shown below have been computed for the values of parameters mentioned in Table 1 unless specified along with the figures. The profiles for interdependent Ca^{2+} and IP_3 concentration and insulin secretion have been plotted.

Figure 1 depicts the distribution of Ca^{2+} and IP_3 at various time and positional instants. Figure 1A exhibits the distribution of Ca^{2+} concentration with respect to space at time $t=0, 5, 20, 50$ and 10 sec respectively. Due to the emission of Ca^{2+} ions, the spatial and temporal profile of $[Ca^{2+}]$ reaches the maximum near the source ($x=0$ μm). Figure 1A shows that the Ca^{2+} concentration decreases as we get farther from the source (from $x=0$ to $x=10$ μm). The phenomenon occurs due to the functioning of the SERCA pump, PMCA pump and binding of Ca^{2+} ions with free buffers. The Fig. 1B shows that as time passes, the concentration of Ca^{2+} rises and reaches a stable state after 150 msec. Oscillations can also be seen at the initial position due to heavy source influx. Because source channels such as ER leak, IP_3 channel and VGCC open, Ca^{2+} ions begin to release and Ca^{2+} rises in the cytosol, the temporal $[Ca^{2+}]$ rises with time at different sites in space.

Figure 1C displays the concentration of IP_3 with respect to space at time $t=0, 5$ msec, $20, 50$ and 10 sec respectively. The IP_3 concentration decreases with the distance as seen in Fig. 1C. IP_3 profile is initially non-linear but this non-linearity reduces with respect to time and becomes nearly linear over a period of time as the multiple IP_3 dynamics processes achieve equilibrium. The IP_3 molecules connect near the IP_3R at different points in time, maintaining the boundary concentration. The IP_3 distribution in a β -cell with respect to space at $x=0, 2.5, 5, 7.5$ and 10 μm is shown in Fig. 1D. Temporal concentration of IP_3 increases with increase in time at various positions as IP_3 molecules bind with IP_3R and start releasing the ER Ca^{2+} ions into the cytosol.

Figure 2 exhibits the variation in Ca^{2+} profile for different values of EGTA $0, 10, 20$ and 50 μM respectively along with the space and time. When no buffer is present, the Ca^{2+} concentration is higher at the beginning node and declines rapidly to achieve the baseline calcium concentration of 0.1 μM along with the space as shown in Fig. 2A. The concentration of Ca^{2+} drops as the buffer concentration rises and thus the background concentration is being achieved at an early stage which cause the change in nature of the curves. This occurs as a result of free calcium ions binding to free buffers. Figure 2B shows that the temporal profile of Ca^{2+} rises over time and reaches steady state sooner for greater buffer values in the cell.

Figure 3 exhibits the influence of BAPTA buffer on Ca^{2+} ions inside the cytosol with respect to space and time. The

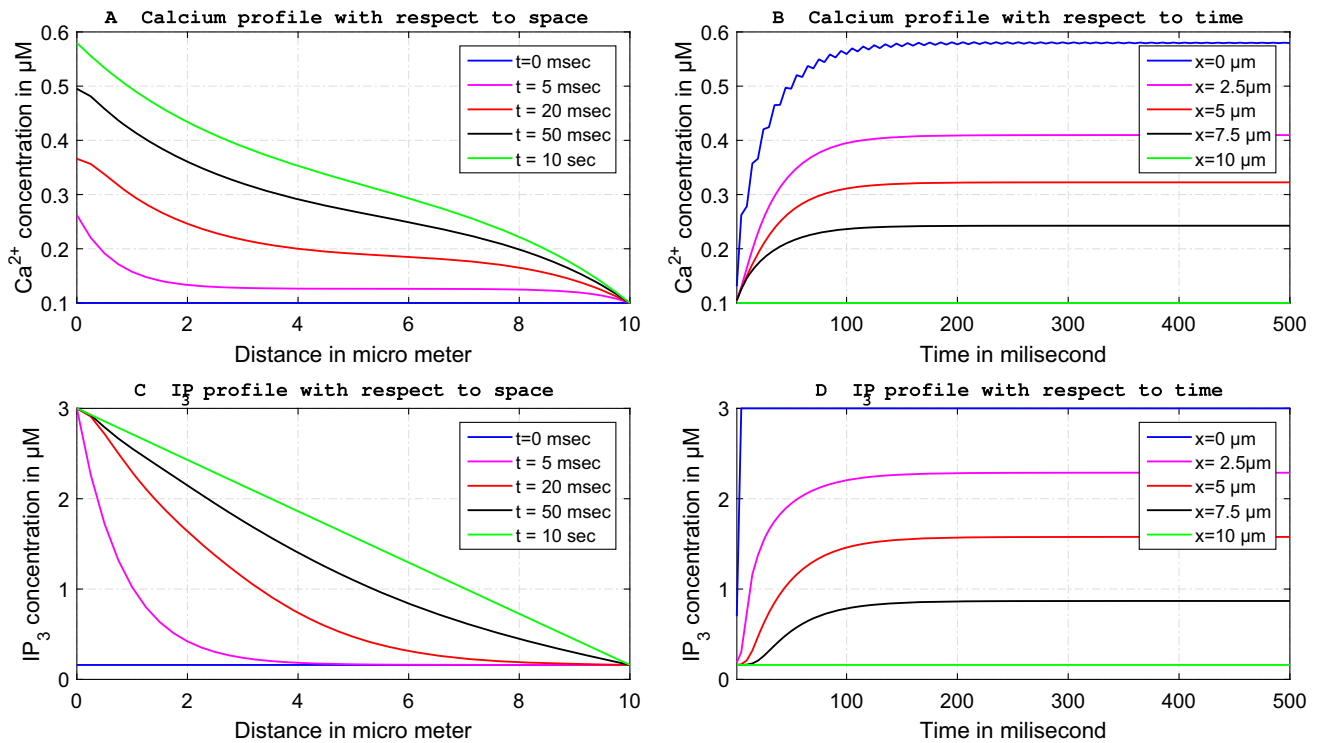


Fig. 1 Interdependent Ca^{2+} and IP_3 dynamics in presence of ER leak, SERCA, IP_3R , PMCA and VGCC in normal conditions (Table 1)

BAPTA is a fast exogenous buffer that binds the calcium ions faster than the EGTA buffer. From Fig. 3A, it can be observed that a slight change in the concentration of BAPTA buffer can lead to a significant variation in calcium concentration. This

phenomenon happened due to the high association rate of BAPTA buffer. The curves achieve the steady state early for the high value of BAPTA and delay can be observed in the steady state for a low value of BAPTA. Thus, the non-linearity

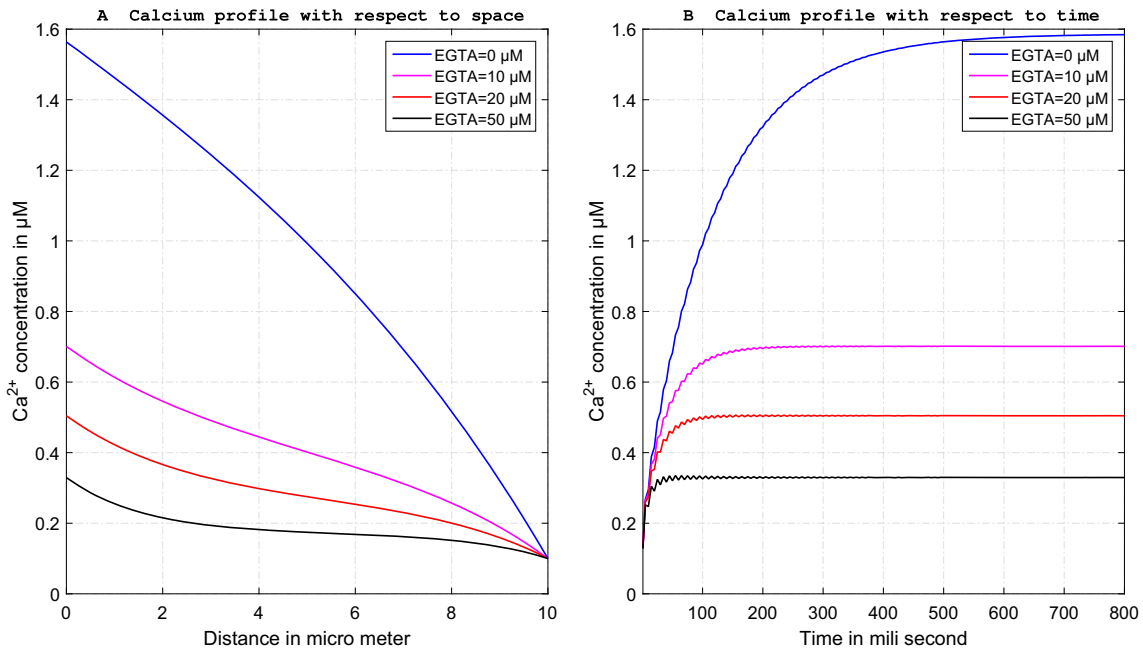


Fig. 2 Ca^{2+} profile for different values of EGTA buffer in presence of ER leak, SERCA, IP_3R , PMCA and VGCC for time $t=50\text{ msec}$ and distance $x=0\text{ }\mu\text{m}$

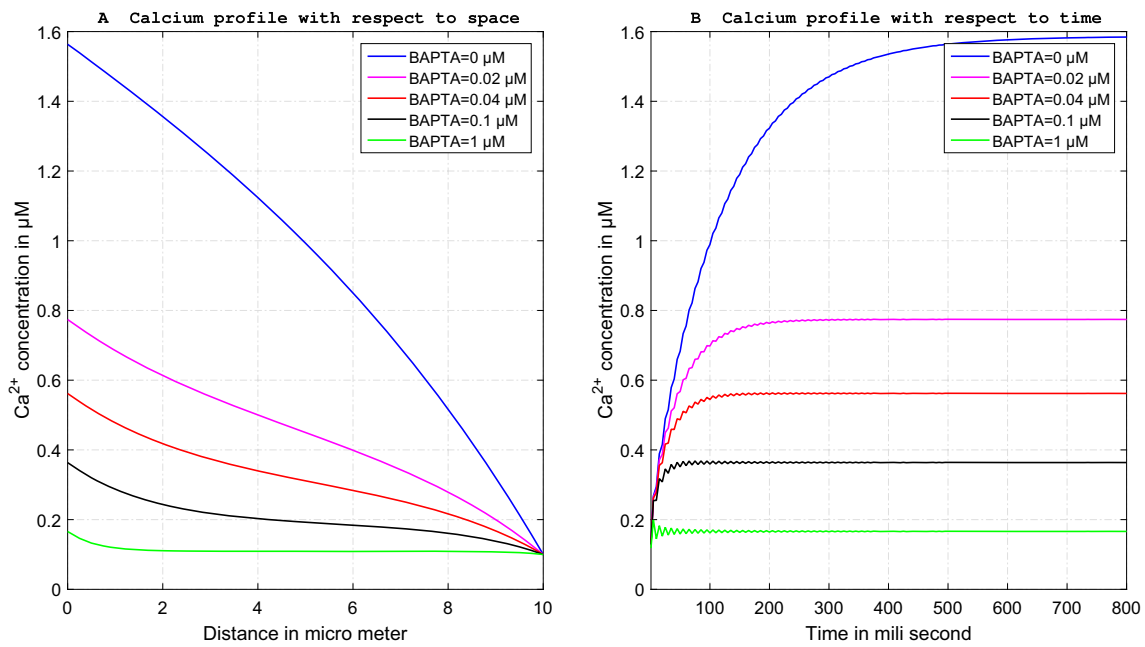


Fig. 3 Ca^{2+} profile for different values of BAPTA buffer in presence of ER leak, SERCA, IP_3R , PMCA and VGCC for time $t=50\text{ msec}$ and distance $x=0\ \mu\text{m}$

of the curves varies as the concentration of the BAPTA buffer increases. Figure 3B depicts the changes in calcium concentration with respect to time for different values of buffer. When the buffer is high the calcium increases slowly with time and for the low value of buffer concentration calcium increases quickly with time.

The impact of source influx on calcium profile with regard to space and time is depicted in Fig. 4A and B respectively. When the source influx grows from 20 to 50 pA at a certain time and distance, Ca^{2+} concentration rises. It is the major factor for increasing or reducing the concentration of calcium in a β -cell to achieve the appropriate amount of Ca^{2+} .

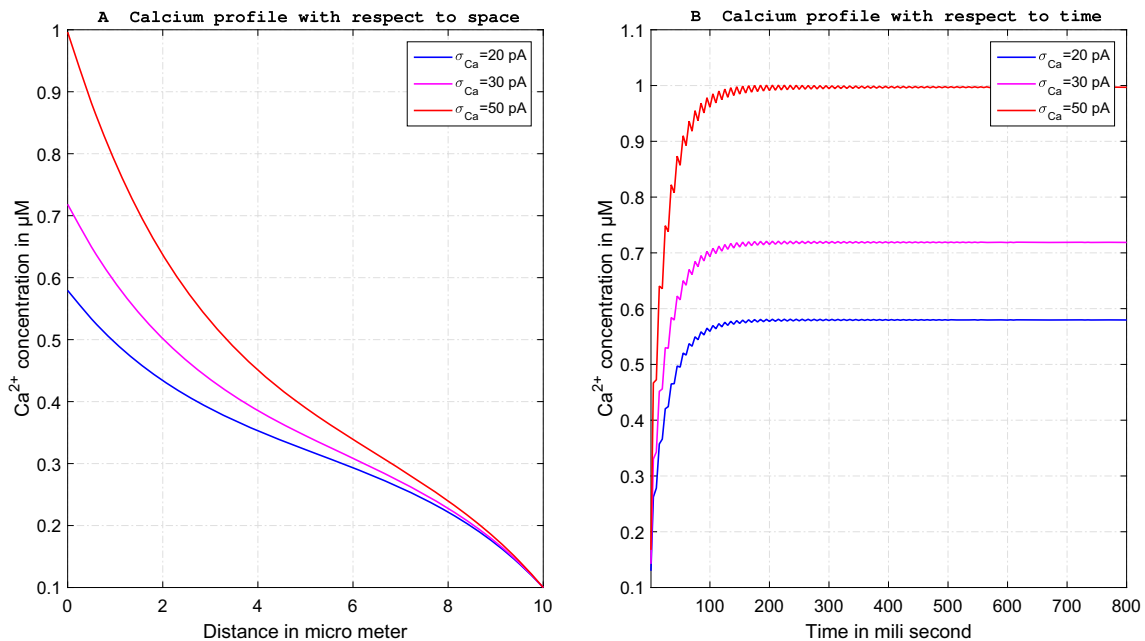


Fig. 4 Ca^{2+} profile for different values of source influx in presence of ER leak, SERCA, IP_3R , PMCA and VGCC for time $t=50\text{ msec}$ and distance $x=0\ \mu\text{m}$

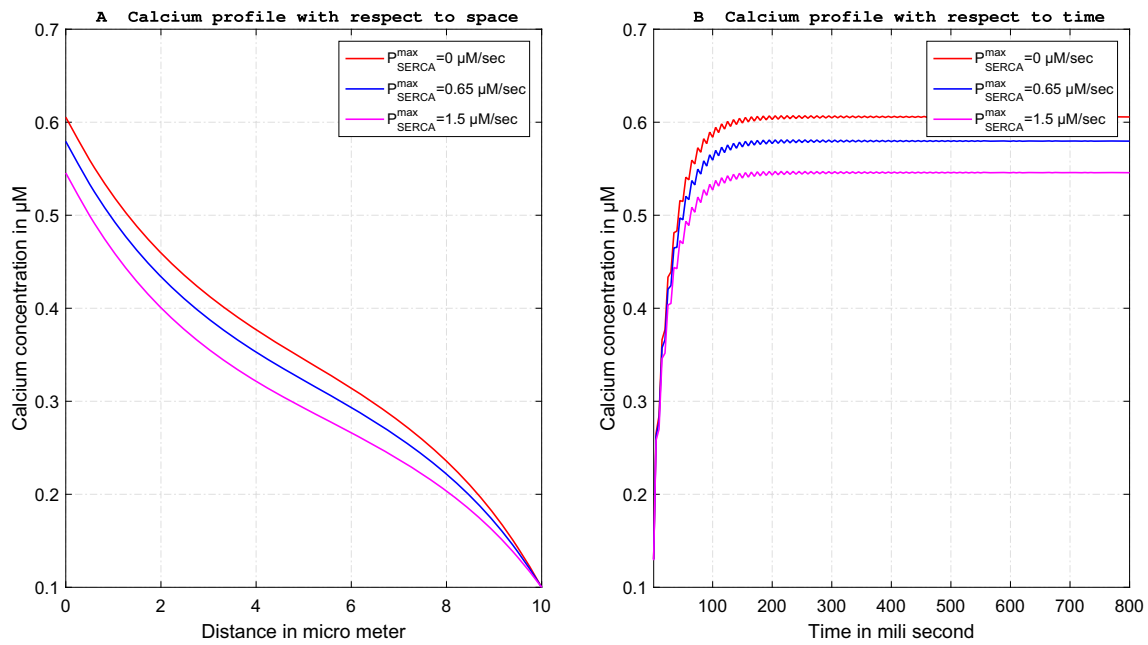


Fig. 5 Ca^{2+} profile for different values of maximum pumping rate of SERCA in presence of ER leak, IP_3R , PMCA and VGCC for time $t=50$ msec and distance $x=0 \mu\text{m}$ (EGTA= $15 \mu\text{M}$ and $\sigma_{Ca}=20 \text{ pA}$)

The spatio temporal changes in calcium profile for distinct values of maximum pumping rate of SERCA 0, 0.65, $1.5 \mu\text{Msec}^{-1}$ respectively are shown in Fig. 5. Because the SERCA transports Ca^{2+} from cytosol to ER for normal β -cell activity, the Ca^{2+} concentration drops as the pumping

rate of SERCA rises. In the β -cell, the Ca^{2+} concentration reaches its maximum level when a SERCA pump is absent.

Figure 6A and B show the changes in Ca^{2+} profile in the presence and absence of PMCA for space and time respectively. The concentration of calcium in Fig. 6A is highest at

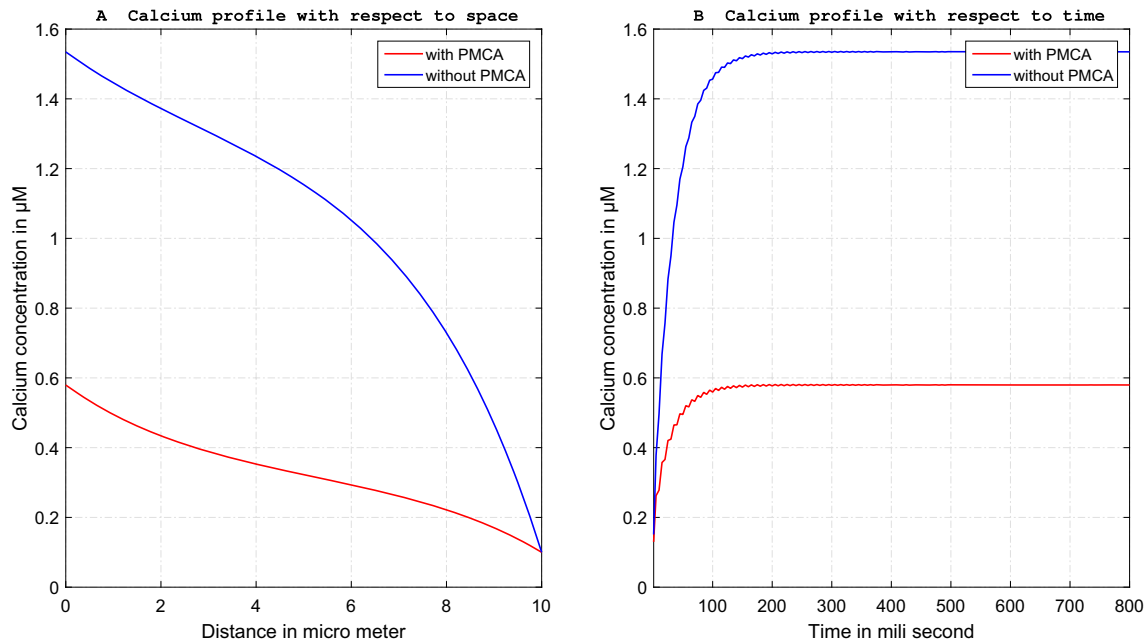


Fig. 6 Ca^{2+} profile with and without PMCA in presence of ER leak, SERCA, IP_3R and VGCC for time $t=50$ msec and distance $x=0 \mu\text{m}$ (EGTA= $15 \mu\text{M}$ and $\sigma_{Ca}=20 \text{ pA}$)

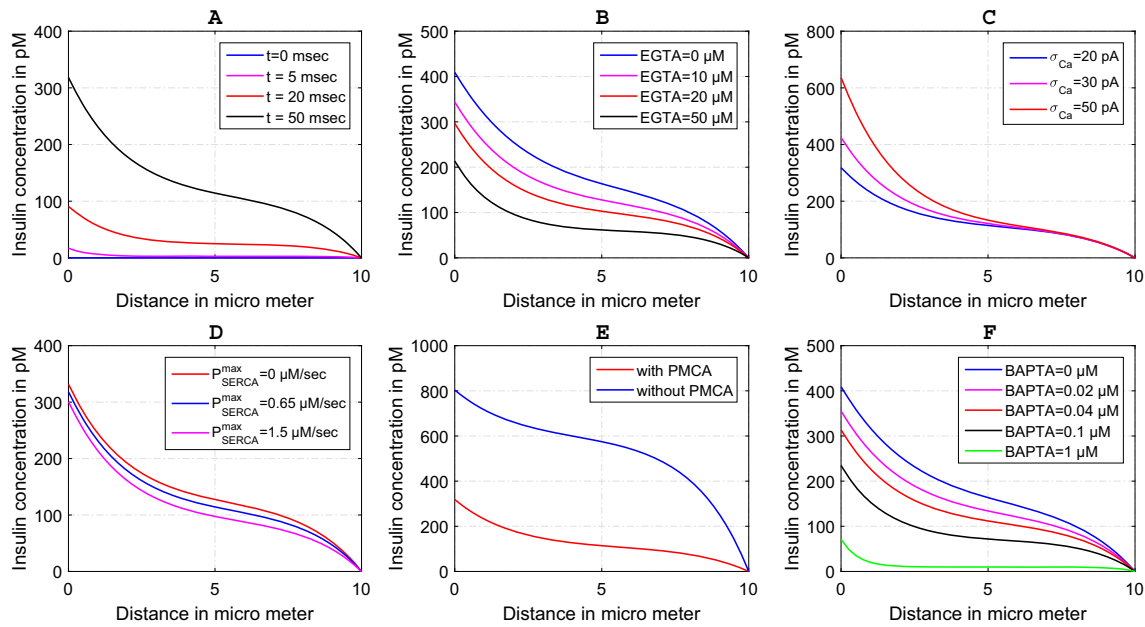


Fig. 7 Insulin profile for different instant of time, EGTA buffer, source influx, SERCA pump rate, PMCA and BAPTA buffer respectively at $x=0 \mu m$

the source $x=0 \mu m$ in absence of PMCA and decreases as the distance grows. However, in case of active PMCA the concentration of calcium is low. This phenomenon occurs because PMCA extracts the extra Ca^{2+} from the cytosol to the extracellular space. In the absence of PMCA, the calcium inclusion mechanism (like VGCC, ER leak and IP3 receptor) plays a dominating role and the Ca^{2+} profile elevates.

Due to the diffusion process, these free calcium ions diffuse over longer distances and attain steady state with a delay. Figure 6B shows the calcium profile for time in absence and presence of PMCA.

Figure 7 exhibits the insulin concentration with respect to space by varying the time, EGTA buffer concentration, source influx value, SERCA pump rate, PMCA pump rate

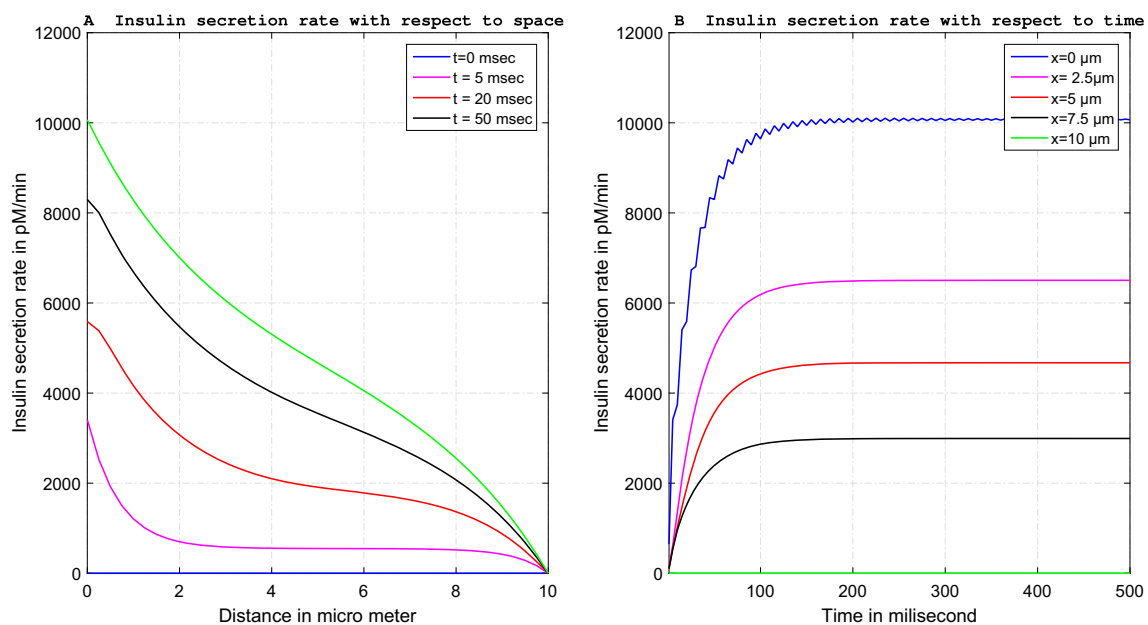


Fig. 8 Insulin secretion rate with respect to space and time for $\sigma_{Ca}=20 pA$, $[B_i]_{\infty}=15 \mu M$, $D_{Ca}=200 \mu m^2 sec^{-1}$ at time $t=50 msec$ and distance $x=0 \mu m$

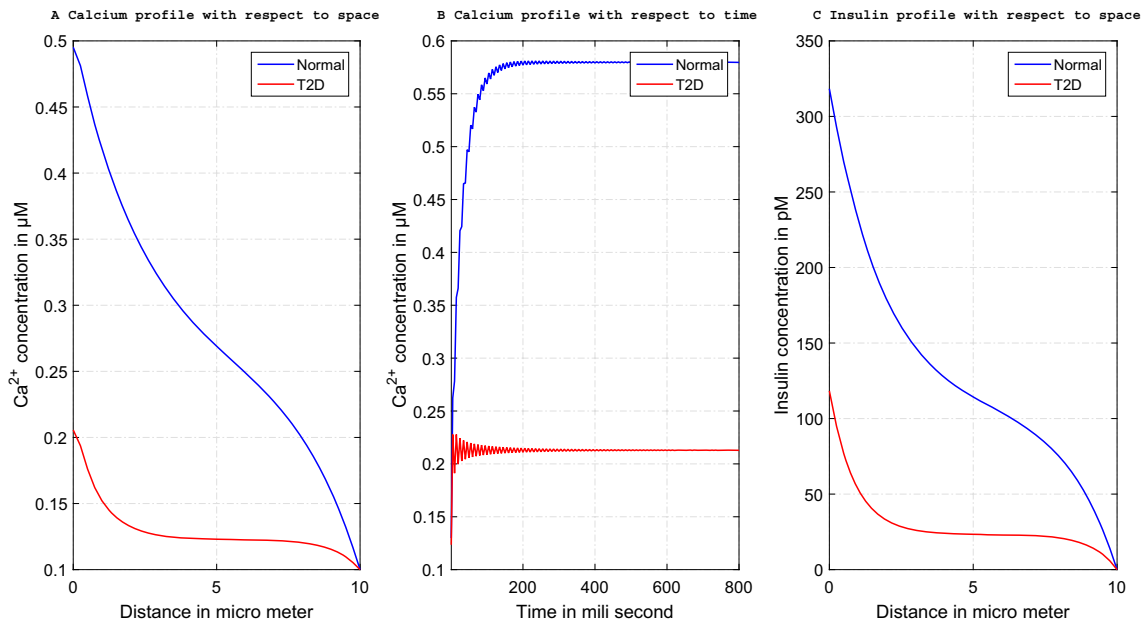


Fig. 9 Calcium and Insulin profile in case of normal and Type-2 diabetes associated with EGTA buffer in presence of ER leak, SERCA, IP_3R , PMCA and VGCC

and BAPTA buffer concentration respectively in β -cells. The insulin concentration throughout space is represented in Fig. 7A for different positions in time $t=0, 5, 20$ and 50 msec. In normal conditions, the insulin concentration almost lies within the expected range as given by Wang et al. (2013). Insulin concentration is highest at $x=0$ μm and gradually declines along the space dimension as shown in Fig. 7A. Insulin concentration follows the same pattern as the calcium

profile. This is simply due to the fact that insulin concentration is influenced by calcium levels. When the cell's Ca^{2+} concentration is greater than 0.1 μM , insulin is constantly secreted and the rate of secretion is determined by the cell's sensitivity. However, because excessive calcium is toxic, the concentration of calcium within the cell cannot remain high indefinitely. As a result, the calcium control system reduces calcium levels, causing insulin secretion to cease. This means

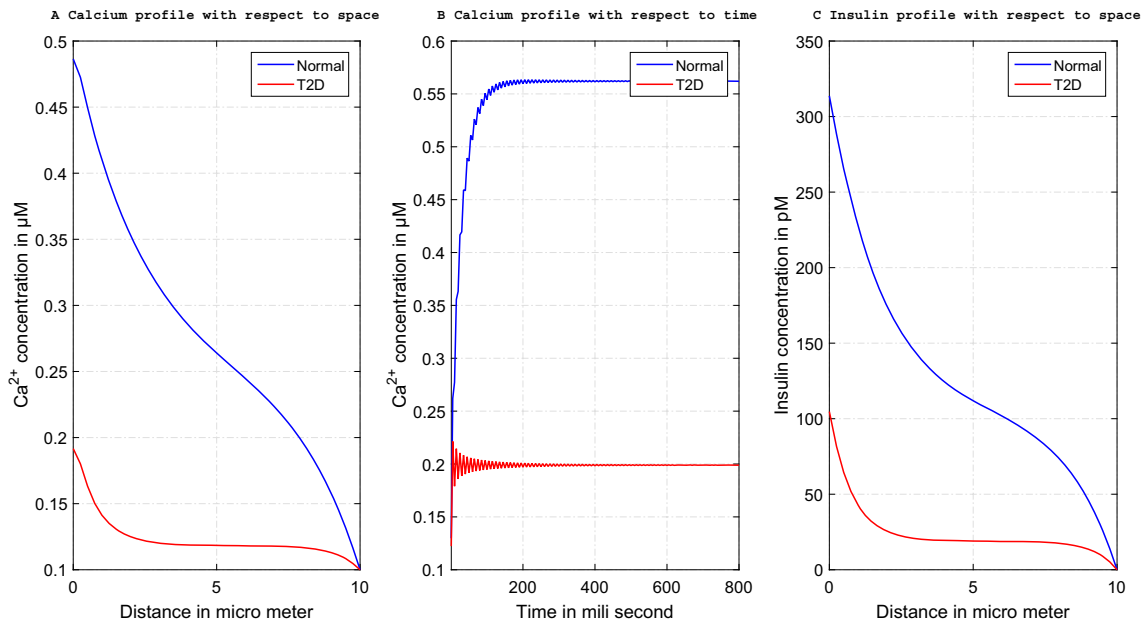


Fig. 10 Calcium and Insulin profile in case of normal and Type-2 diabetes associated with BAPTA buffer in presence of ER leak, SERCA, IP_3R , PMCA and VGCC

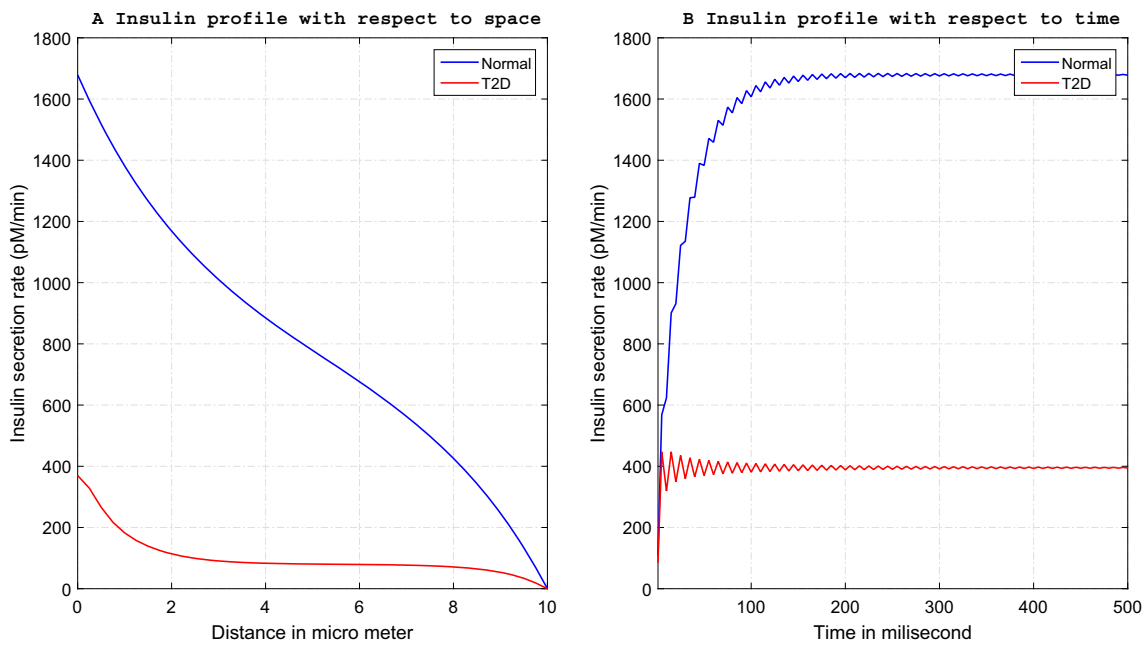


Fig. 11 Secretion Rate of Insulin in case of normal and Type-2 diabetes associated with EGTA buffer in presence of ER leak, SERCA, IP_3R , PMCA and VGCC

that insulin secretion occurs in the cell in a switch-on/switch-off fashion. This is also evident from the fact that at the same time all the insulin granules are not in secretion mode. Only 100 of the 10,000 granules in a β -cell are actively secreting insulin (Bratanova-Tochkova et al. 2002). This indicates that the β -cell become sensitive to insulin release in batches

and they secrete insulin in an on/off manner. The Fig. 7B exhibits the spatial variation in insulin concentration for different values of EGTA 0, 10, 20, 50 μM respectively. It is observed that insulin shows the same behaviour as seen in calcium Fig. 2A. Thus, in a β -cell the buffer's effect on calcium signaling is passed in the same proportion to

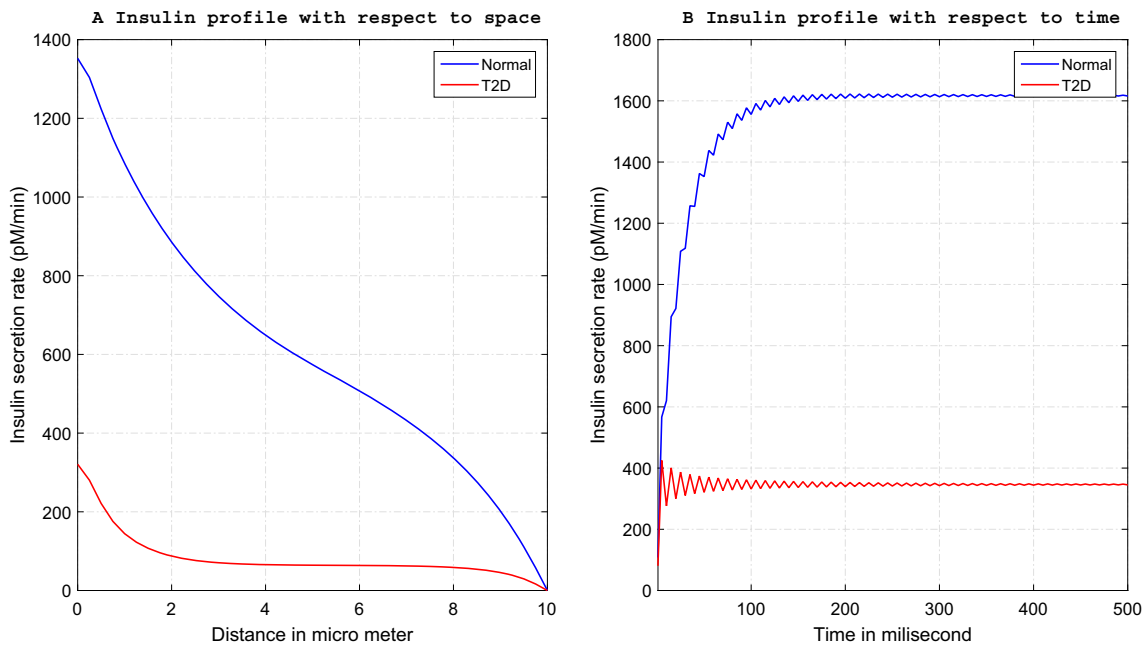


Fig. 12 Secretion Rate of Insulin in case of normal and Type-2 diabetes associated with BAPTA buffer in presence of ER leak, SERCA, IP_3R , PMCA and VGCC

Table 2 Analysis of error for calcium concentration when $x=0 \mu M$ for 30 and 40 elements

Time	N=30	N=40	Absolute Error	Relative % Error
0.1 sec	0.557239211	0.556150998	0.001088213	0.195286501 %
0.2 sec	0.574825081	0.573961768	0.000863313	0.150187055 %
0.5 sec	0.576515031	0.576293888	0.000221143	0.03835854%
1 sec	0.57658363	0.576614652	0.000031	0.005380342%

insulin concentration. The insulin concentration decreases with the increase in values of buffer. This occurs due to binding of buffers with free calcium, reducing the cytosolic calcium which in turn brings down the insulin concentration. Figure 7C displays the insulin concentration for different values of source influx 20, 30, 50 pA respectively at a particular time and position. Insulin concentration increases with an increase in source influx as insulin concentration is dependent on cytosolic calcium as shown in Fig. 4A. Figure 7D shows the spatial variation for various choices of the maximum pumping rate of SERCA 0, 0.65 and $1.5 \mu M sec^{-1}$ of insulin concentration. The Fig. 7D shows that the concentration of insulin is high for a low value of the pumping rate of SERCA and as the pumping rate increases, insulin concentration decreases with respect to space. Figure 7E shows the influence of PMCA on insulin concentration. In the presence of PMCA the insulin concentration is low as the concentration of calcium is low, while in case of inactive PMCA the concentration of insulin is higher. The effect of BAPTA buffer on insulin concentration can be observed from the Fig. 7F. It is evident from the figure that the concentration of insulin is inversely proportional to the BAPTA buffer concentration.

The rate of insulin secretion for both space and time is shown in Fig. 8. The curves for the various instants of time for space are shown in Fig. 8A. The figure shows how the secretion rate decreases with increasing distance and grows with time, but after a while, it reaches a stable state and no additional elevation is seen Fig. 8B. Due to the existence of source terms, oscillations for the secretion rate at $x=0 \mu m$ can be observed.

Figures 9 and 10 show the calcium and insulin concentration profile for EGTA and BAPTA buffer in case of normal and Type-2 diabetic conditions. It can be seen in Figs. 9 and 10, that both calcium and insulin profiles decreased significantly. The BAPTA buffer has a high association rate which causes it to decrease the level more markedly

even when added in little amounts as compared to EGTA buffer. The change in the nature of the curves can also be observed in the Figs. 9 and 10 because when buffers are added in a small amount, more calcium ions are free in the cytosol, which diffuses up to a more significant distance inside the cell but when buffers are added into higher amount it binds the calcium ions which slow down the diffusion process and the steady state is achieved earlier. Since the insulin profile is calcium-dependent, it shows similar behavior. Figures 11 and 12 represent the insulin secretion rate for EGTA and BAPTA buffer in case of normal and Type-2 diabetic conditions. A significant reduction has been observed from the figures in secretion rate of insulin in case of Type-2 diabetes. The oscillations are observed in Figs. 9B, 10B, 11B and 12B for higher values of buffer. This implies that the calcium regulation mechanisms take some time to achieve balance among the sub processes and reach steady state after some time. By changing the buffer values almost 60 % reduction in the insulin secretion rate can be observed, which is the case of Type-2 diabetes. These insights of various mechanisms, their disturbances and consequential effects can be useful for treatment of Type 2 diabetes.

Conclusion

In conclusion, a systems biology model for describing the interdependency of Ca^{2+} and IP_3 in a pancreatic β -cell is proposed. The function of SERCA pumps, buffer, leak, IP_3R , PMCA pump and VGCC in forming the fundamental dynamical landscape of our model of triggered calcium responses in the β -cell is studied using computational analyses and simulations. The model has also been framed to investigate the effects of system dynamics Ca^{2+} and IP_3 on Ca^{2+} -dependent insulin secretion in a β -cell. The linear

Table 3 Analysis of error for IP_3 concentration when $x=0.25 \mu M$ for 30 and 40 elements

Time	N=30	N=40	Absolute Error	Relative % Error
0.1 sec	2.904331472	2.934696856	0.030365384	1.034702588 %
0.2 sec	2.907435655	2.933541049	0.026105394	0.889893591 %
0.5 sec	2.90544686	2.92963082	0.02418396	0.825495154 %
1 sec	2.90527074	2.929007576	0.023736836	0.810405423 %

Table 4 Comparison of $[Ca^{2+}]$ profile at $t=50$ sec

Distance (μm)	$[Ca^{2+}]$ (Wagner et al. 2004)	$[Ca^{2+}]$ (Present Work)
0	1.35	1.350029674
2	1.192540688	1.190689045
4	1.080154535	1.064165408
6	0.937748913	0.905002462
8	0.670328457	0.630870015
10	0.1	0.1

finite elements and Crank-Nicolson schemes are used respectively with respect to space and time coordinates. The Ca^{2+} concentration profiles have been presented in response to varied buffer concentrations, varying amplitudes of Ca^{2+} source, active and inactive SERCA pump, ER leak and PMCA pump. The numerical solution results are used to arrive at the following basic conclusions:

- (i) With increasing buffer concentration, the peak value of Ca^{2+} concentration in a β -cell falls. This is because the elevated buffer concentration binds the Ca^{2+} , lowering the Ca^{2+} concentration in the cytosol. The EGTA and BAPTA are exogenous in nature and are used to slow down the diffusion process by binding with free cytosolic calcium ions.
- (ii) In the case of active VGCC, IP_3R and ER leak, the amount of intracellular Ca^{2+} is larger than in the case of inactive VGCC, IP_3R and ER leak. This means that VGCC, IP_3R and ER leak all help the cell to increase Ca^{2+} concentration when the cell requires it.
- (iii) High source influx combined with lower SERCA and PMCA pump values can lead to an increase in Ca^{2+} and IP_3 concentration profiles, which boosts insulin secretion.
- (iv) The model is effective in providing the response time of the cell in achieving the maximal secretion rate for insulin.
- (v) The relative percentage errors have been computed to estimate the accuracy of the model and the mesh sensitivity for the finite element procedure given in Tables 2 and 3. The maximum percentage errors were found to be 0.195 % for Ca^{2+} concentration and 1.035 % for

IP_3 concentration. The maximum accuracy were found to be 99.805 % for Ca^{2+} concentration and 98.9650 % for IP_3 concentration. Thus, it can be concluded from the obtained results that the method is mesh independent. The spectral radius was estimated and found to be 0.999, which is less than 1, which supports the assertion that the solution approach is stable.

- (vi) The present model has been found to be in good agreement with Wagner et al. (2004). For validation purpose, the Ca^{2+} and IP_3 concentrations at some points for $t=50$ sec have been observed from the work of Wagner et al. (see figure 3 2004) and from the present work. The observed data is given in Tables 4 and 5. Further, the root mean square error for Ca^{2+} and IP_3 has also been calculated and found to be 0.0241 and 4.23E-06 respectively, which are almost negligible.

The following novel conclusions are drawn on the basis of numerical results:

- (i) The disturbances/changes in the system dynamics of Ca^{2+} and IP_3 leads to changes in insulin secretion.
- (ii) The changes in source influx causing changes in Ca^{2+} levels, thereby causes changes in insulin secretion. The decrease in source influx causes lower secretion rate of insulin. Insulin release rises as the source inflow rises, potentially causing β -cell overstimulation and resulting in obesity, cardiovascular disease, hypertension and other metabolic problems (Sprietsma and Schuitemaker 1994).

Table 5 Comparison of $[IP_3]$ profile at $t=50$ sec

Distance (μm)	$[IP_3]$ (Wagner et al. 2004)	$[IP_3]$ (Present Work)
0	0.5	0.5
2	0.430982023	0.43098468
4	0.362510677	0.362515755
6	0.294550377	0.294556528
8	0.227063092	0.227067657
10	0.16	0.16

- (iii) The changes in buffering activity causes changes in Ca^{2+} levels and thus leads to changes in insulin secretion levels. The higher rate of buffering causes decrease in insulin secretion. Insulin levels have been found to be low in both Type 1 and Type 2 diabetes (Jaberi-Douraki et al. 2015; Rorsman 2005). In normal settings, insulin secretion rate ranges between 400 and 1600 $pmol/min$ (Rorsman 2005). The rate of insulin secretion remains almost within this range, as shown in Fig. 8.
- (iv) The model is effective to provide the role of buffers in normal and diabetic conditions. Figures 11 and 12 show the insulin secretion rate in case of non-diabetic and diabetic conditions. Almost 60% reduction can be observed in Figs. 11 and 12 in secretion rate of insulin by changing the buffers concentration which is the case of Type-2 diabetes (Rorsman and Braun 2013). It can be concluded from the observation that due to high association rate of BAPTA buffers, low amount of BAPTA can be significant to achieve the normal range. Whereas high amount of EGTA buffer is required to achieve the same. The obtained results are in good agreement with the results obtained by Pertusa et al. (1999).
- (v) The proposed model is novel as no researcher in the past had studied the impact of interdependent dynamics of Ca^{2+} and IP_3 on insulin secretion. The past studies reported are mostly for independent Ca^{2+} dynamics affecting insulin secretion which provide limited information. The balancing effect of Ca^{2+} and IP_3 on each other gives better insights of the impact of system dynamics on insulin secretion in normal and diabetic cell. The significant changes in insulin secretion take place due to Type-1 and Type-2 diabetes as revealed by the results.

According to the results, the interdependent Ca^{2+} and IP_3 dynamics in a β -cell are significantly influenced by the buffers, source influx, SERCA, leak, PMCA and VGCC, which are required for maintaining the cell's structure and function. Any disruption in these factors in a β -cell can result in major diseases like obesity, diabetes and hypertension. The proposed model provides us with useful information that may be used to develop treatment and diagnosis for a variety of diseases. The mathematical model proposed here is highly adaptable, as it allows for the inclusion of minute parameter details. These kinds of mathematical models can be utilised to create crucial data for Ca^{2+} management.

Author Contributions V.: Literature Survey, Writing-Original draft preparation, Conceptualization, Methodology, Investigation, Matlab Program. N.A.: Visualization, Supervision, Reviewing and Editing. All authors discussed the results and contributed to the final manuscript.

Funding Not applicable.

Availability of data and materials Not applicable.

Declaration

Statement of Conflict of Interest There are no conflicts of interest declared by the authors.

Ethical Approval There are no animal trials in the study, which eliminates the requirement for ethical review. It is entirely quantitative and computational.

Appendix

The finite element approach was used to solve the model described by the Eqs. 1 to 22 along spatial dimension. Since the present study is focused on one-dimensional model, so the linear shape function is the best fit to discretized the domain. As linear shape elements are good enough to reduce the complexity of the model and make it computationally tractable. Also, by increasing the number of elements desired accuracy can be achieved, as mentioned in the Table 3. Thus, for each element, the following is the linear shape function of Ca^{2+} and IP_3 concentration:

$$u^{(e)} = c_1^{(e)} + c_2^{(e)}x, \quad (24)$$

$$v^{(e)} = d_1^{(e)} + d_2^{(e)}x, \quad (25)$$

$$u^{(e)} = p^T c^{(e)}, \quad v^{(e)} = p^T d^{(e)}, \quad (26)$$

where

$$p^T = [1 \quad x],$$

$$c^{(e)} = [c_1^{(e)} \quad c_2^{(e)}]^T,$$

$$d^{(e)} = [d_1^{(e)} \quad d_2^{(e)}]^T.$$

After substituting the nodal values in Eq. 26, we get;

$$\begin{bmatrix} u_1 \\ u_2 \end{bmatrix} = \begin{bmatrix} 1 & x_i \\ 1 & x_j \end{bmatrix} \begin{bmatrix} c_1^{(e)} \\ c_2^{(e)} \end{bmatrix},$$

$$\begin{bmatrix} v_1 \\ v_2 \end{bmatrix} = \begin{bmatrix} 1 & x_i \\ 1 & x_j \end{bmatrix} \begin{bmatrix} d_1^{(e)} \\ d_2^{(e)} \end{bmatrix},$$

$$\bar{u}^{(e)} = P^{(e)}c^{(e)}, \quad \bar{v}^{(e)} = P^{(e)}d^{(e)}, \quad (27)$$

$$\bar{u}^{(e)} = \begin{bmatrix} u_1 \\ u_2 \end{bmatrix}, \quad \bar{v}^{(e)} = \begin{bmatrix} v_1 \\ v_2 \end{bmatrix} \quad \text{and} \quad P^{(e)} = \begin{bmatrix} 1 & x_i \\ 1 & x_j \end{bmatrix}. \quad (28)$$

Equation 27 can be re-written as:

$$c^{(e)} = R^{(e)}\bar{u}^{(e)}, \quad d^{(e)} = R^{(e)}\bar{v}^{(e)}, \quad (29)$$

where

$$R^{(e)} = P^{(e)-1}.$$

Using Eqs. 26 and 29, we get

$$u^{(e)} = p^T R^{(e)} \bar{u}^{(e)}, \quad v^{(e)} = p^T R^{(e)} \bar{v}^{(e)}. \tag{30}$$

Discretizing the space into 40 linear elements and linearising the Eqs. 1 and 2, the integral A and B can be expressed in this formulation:

$$A = A_1 - A_2 - A_3 - A_4 + A_5 - A_6, \tag{31}$$

$$B = B_1 - B_2 - B_3 - B_4 + B_5, \tag{32}$$

where

$$A_1 = \frac{1}{2} \int_{x_i}^{x_j} \left(\frac{\partial u^{(e)}}{\partial x} \right)^2 dx, \tag{33}$$

$$A_2 = \frac{a_{11}}{2} \int_{x_i}^{x_j} (u^{(e)})^2 dx, \tag{34}$$

$$A_3 = a_{12} \int_{x_i}^{x_j} u^{(e)} v^{(e)} dx, \tag{35}$$

$$A_4 = a_{13} \int_{x_i}^{x_j} u^{(e)} dx, \tag{36}$$

$$A_5 = \frac{1}{2D_{Ca}} \int_{x_i}^{x_j} \frac{\partial}{\partial t} (u^{(e)})^2 dx, \tag{37}$$

$$A_6 = \frac{\sigma}{D_{Ca}} (u^{(e)})_{x=0}, \tag{38}$$

$$B_1 = \frac{1}{2} \int_{x_i}^{x_j} \left(\frac{\partial v^{(e)}}{\partial x} \right)^2 dx, \tag{39}$$

$$B_2 = \frac{a_{11}}{2} \int_{x_i}^{x_j} (v^{(e)})^2 dx, \tag{40}$$

$$B_3 = a_{12} \int_{x_i}^{x_j} u^{(e)} v^{(e)} dx, \tag{41}$$

$$B_4 = a_{13} \int_{x_i}^{x_j} v^{(e)} dx, \tag{42}$$

$$B_5 = \frac{1}{2D_{IP_3}} \int_{x_i}^{x_j} \frac{\partial}{\partial t} (v^{(e)})^2 dx. \tag{43}$$

After applying all the initial and boundary conditions we get a system of equation given as follows:

$$\frac{dA}{d\bar{u}^{(e)}} = \sum_{e=1}^{40} \bar{Q}^{(e)} \frac{dA^{(e)}}{d\bar{u}^{(e)}} \bar{Q}^{(e)T} = 0, \tag{44}$$

$$\frac{dB}{d\bar{v}^{(e)}} = \sum_{e=1}^{40} \bar{Q}^{(e)} \frac{dB^{(e)}}{d\bar{v}^{(e)}} \bar{Q}^{(e)T} = 0, \tag{45}$$

where

$$\bar{Q}^{(e)} = \begin{bmatrix} 0 & 0 \\ \vdots & \vdots \\ 0 & 0 \\ 1 & 0 \\ 0 & 1 \\ 0 & 0 \\ \vdots & \vdots \\ 0 & 0 \end{bmatrix}, \quad \bar{u} = \begin{bmatrix} u_1 \\ u_2 \\ u_3 \\ \vdots \\ u_{40} \\ u_{41} \end{bmatrix} \quad \text{and} \quad \bar{v} = \begin{bmatrix} v_1 \\ v_2 \\ v_3 \\ \vdots \\ v_{40} \\ v_{41} \end{bmatrix}. \tag{46}$$

The non zero vectors [1, 0] and [0, 1] are located at the i^{th} and j^{th} row of the matrix $\bar{Q}^{(e)}$.

$$[X]_{82 \times 82} \begin{bmatrix} \left[\frac{\partial \bar{u}}{\partial t} \right]_{41 \times 1} \\ \left[\frac{\partial \bar{v}}{\partial t} \right]_{41 \times 1} \end{bmatrix} + [Y]_{82 \times 82} \begin{bmatrix} [\bar{u}]_{41 \times 1} \\ [\bar{v}]_{41 \times 1} \end{bmatrix} = [Z]_{82 \times 1}. \tag{47}$$

X and Y represents the system matrices and Z represents a system vector. Temporal system given in Eq. 47 is solved using Crank-Nicolson scheme and simulated on MATLAB to obtain numerical results.

References

Ainscow EK, Rutter GA (2002) Glucose-stimulated oscillations in free cytosolic ATP concentration imaged in single islet β -cells: evidence for a Ca^{2+} -dependent mechanism. *Diabetes* 51(suppl-1):S162–S170

Berridge MJ, Irvine RF (1984) Inositol trisphosphate, a novel second messenger in cellular signal transduction. *Nature* 312(5992):315–321. <https://doi.org/10.1038/312315a0>

Berridge MJ (2016) The inositol trisphosphate/calcium signaling pathway in health and disease. *Physiological reviews* 96(4):1261–1296. <https://doi.org/10.1152/physrev.00006.2016>

Bhardwaj H, Adlakha N (2022) Radial basis function based differential quadrature approach to study reaction diffusion of Ca^{2+} in T lymphocyte. *International Journal of Computational Methods*. <https://doi.org/10.1142/S0219876222500591>

Boob-Bavnbeek B, Larsen J, Renström E (2008) Systems biology of regulated exocytosis in pancreatic β -cells. Working Paper, Roskilde

Bootman MD, Berridge MJ (1995) The elemental principles of calcium signaling. *Cell* 83(5):675–678

Bratanova-Tochkova TK, Cheng H, Daniel S, Gunawardana S, Liu YJ, Mulvaney-Musa J, Sharp GW (2002) Triggering and augmentation mechanisms, granule pools, and biphasic insulin secretion. *Diabetes* 51(suppl-1):S83–S90. <https://doi.org/10.2337/diabetes.51.2007.S83>

Braun M, Ramracheya R, Bengtsson M, Zhang Q, Karanauskaite J, Partridge C, Rorsman P (2008) Voltage-gated ion channels in human pancreatic β -cells: electrophysiological characterization and role in insulin secretion. *Diabetes* 57(6):1618–1628. <https://doi.org/10.2337/db07-0991>

- Buchwald P (2011) A local glucose-and oxygen concentration-based insulin secretion model for pancreatic islets. *Theoretical biology and medical modelling* 8(1):1–25
- Chay TR, Keizer J (1983) Minimal model for membrane oscillations in the pancreatic β -cell. *Biophys J* 42:181–90. [https://doi.org/10.1016/s0006-3495\(83\)84384-7](https://doi.org/10.1016/s0006-3495(83)84384-7) 57, 358, 358, 359
- Crank J (1979) *The mathematics of diffusion*. Oxford University Press
- Das PN, Halder S, Bairagi N, Chatterjee S (2020) Delay in ATP-dependent calcium inflow may affect insulin secretion from pancreatic beta-cell. *Appl Math Model* 84:202–221. <https://doi.org/10.1016/j.apm.2020.03.030>
- Paul A, Das PN, Chatterjee S (2022) A minimal model of glucose-stimulated insulin secretion process explores factors responsible for the development of type 2 diabetes. *Appl Math Model* 108:408–426. <https://doi.org/10.1016/j.apm.2022.03.035>
- De Young GW, Keizer J (1992) A single-pool inositol 1, 4, 5-trisphosphate-receptor-based model for agonist-stimulated oscillations in Ca^{2+} concentration. *Proceedings of the National Academy of Sciences* 89(20):9895–9899. <https://doi.org/10.1073/pnas.89.20.9895>
- Decrock E, De Bock M, Wang N, Gadicherla AK, Bol M, Delvaeye T, Leybaert L (2013) IP_3 , a small molecule with a powerful message. *Biochimica et Biophysica Acta (BBA)-Molecular Cell Research* 7:1772–1786. <https://doi.org/10.1016/j.bbamer.2012.12.016>
- Dupont G, Erneux C (1997) Simulations of the effects of inositol 1, 4, 5-trisphosphate 3-kinase and 5-phosphatase activities on Ca^{2+} oscillations. *Cell calcium* 22(5):321–331. [https://doi.org/10.1016/S0143-4160\(97\)90017-8](https://doi.org/10.1016/S0143-4160(97)90017-8)
- Fridlyand LE, Tamarina N, Philipson LH (2010) Bursting and calcium oscillations in pancreatic β -cells: specific pacemakers for specific mechanisms. *Am J Physiol-Endocrinol Metab* 299(4):E517–E532. <https://doi.org/10.1152/ajpendo.00177.2010>
- Fridlyand LE, Tamarina N, Philipson LH (2003) Modeling of Ca^{2+} flux in pancreatic β -cells: role of the plasma membrane and intracellular stores. *Am J Physiol-Endocrinol Metab* 285(1):E138–E154. <https://doi.org/10.1152/ajpendo.00194.2002>
- Goforth PB, Bertram R, Khan FA, Zhang M, Sherman A, Satin LS (2002) Calcium-activated K^+ channels of mouse β -cells are controlled by both store and cytoplasmic Ca^{2+} experimental and theoretical studies. *J Gen Physiol* 120(3):307–322. <https://doi.org/10.1085/jgp.20028581>
- Gopel SO, Kanno T, Barg S, Eliasson L, Galvanovskis J, Renstrom E, Rorsman P (1999) Activation of Ca^{2+} -dependent K^+ channels contributes to rhythmic firing of action potentials in mouse pancreatic β -cells. *J Gen Physiol* 114(6):759–770. <https://doi.org/10.1085/jgp.114.6.759>
- Higgins ER, Cannell MB, Sneyd J (2006) A buffering SERCA pump in models of calcium dynamics. *Biophysical J* 91(1):151–163. <https://doi.org/10.1529/biophysj.105.075747>
- Idevall-Hagren O, Tengholm A (2020) Metabolic regulation of calcium signaling in beta cells. In *Seminars in Cell & Developmental Biology*, Vol. 103. Academic Press, pp. 20–30. <https://doi.org/10.1016/j.semcdb.2020.01.008>
- Jaberi-Douraki M, Schnell S, Pietropaolo M, Khadra A (2015) Unraveling the contribution of pancreatic beta-cell suicide in autoimmune type 1 diabetes. *J Theor Biol* 375:77–87. <https://doi.org/10.1016/j.jtbi.2014.05.003>
- Jha A, Adlakha N (2014) Finite element model to study the effect of exogenous buffer on calcium dynamics in dendritic spines. *Int J Model Simul Sci Comput* 5(02):1350027. <https://doi.org/10.1142/S179396231350027X>
- Jha A, Adlakha N, Jha BK (2016) Finite element model to study effect of Na^+ - Ca^{2+} exchangers and source geometry on calcium dynamics in a neuron cell. *J Mech Med Biol* 16(02):1650018. <https://doi.org/10.1142/S0219519416500184>
- Jha BK, Adlakha N, Mehta MN (2013) Two-dimensional finite element model to study calcium distribution in astrocytes in presence of VGCC and excess buffer. *International Journal of Modeling, Simulation, and Scientific Computing* 4(02):1250030. <https://doi.org/10.1142/S1793962312500304>
- Keizer J, Magnus G (1989) ATP-sensitive potassium channel and bursting in the pancreatic beta cell. A theoretical study. *Biophys J* 56(2):229–242. [https://doi.org/10.1016/S0006-3495\(89\)82669-4](https://doi.org/10.1016/S0006-3495(89)82669-4)
- Klec C, Ziomek G, Pichler M, Malli R, Graier WF (2019) Calcium signaling in β -cell physiology and pathology: a revisit. *Int J Mol Sci* 20(24):6110. <https://doi.org/10.3390/ijms20246110>
- Kothiya A, Adlakha N (2022) Model of Calcium Dynamics Regulating IP_3 and ATP Production in a Fibroblast Cell. *Advances in Systems Science and Applications* 22(3), 49–69. <https://doi.org/10.25728/assa.2022.22.3.1219>
- Kothiya AB, Adlakha, N (2023) Cellular nitric oxide synthesis is affected by disorders in the interdependent Ca^{2+} and IP_3 dynamics during cystic fibrosis disease. *J Biol Phys* 1–26
- Magnus G, Keizer J (1997) Minimal model of beta-cell mitochondrial Ca^{2+} handling. *Am J Physiol-Cell Physiol* 273(2):C717–C733. <https://doi.org/10.1152/ajpcell.1997.273.2.C717>
- Misler S, Barnett DW, Gillis KD, Pressel DM (1992) Electrophysiology of stimulus-secretion coupling in human β -cells. *Diabetes* 41(10):1221–1228. <https://doi.org/10.2337/diab.41.10.1221>
- Naik PA, Pardasani KR (2014) Finite Element Model to Study Effect of Na^+/K^+ Pump and Na^+/Ca^{2+} Exchanger on Calcium Distribution in Oocytes in Presence of Buffers. *Asian J Math & Stat* 7(1):21
- Naik PA, Pardasani KR (2019) Three-dimensional finite element model to study effect of RyR calcium channel, ER leak and SERCA pump on calcium distribution in oocyte cell. *Int J Comput Methods* 16(01):1850091. <https://doi.org/10.1142/S0219876218500913>
- Naik PA, Zu J (2020) Modeling and simulation of spatial-temporal calcium distribution in T lymphocyte cell by using a reaction-diffusion equation. *J Bioinforma Comput Biol* 18(02):2050013. <https://doi.org/10.1142/S0219720020500134>
- Panday S, Pardasani KR (2013) Finite element model to study effect of advection diffusion and Na^+/Ca^{2+} exchanger on Ca^{2+} distribution in oocytes. *J Med Imaging Health Inform* 3(3):374–379. <https://doi.org/10.1166/jmihi.2013.1184>
- Panday S, Pardasani KR (2013) Finite element model to study effect of buffers along with leak from er on cytosolic Ca^{2+} distribution in oocyte. *IOSR J Math (IOSR-JM)* ISSN 2278–5728
- Pawar A, Pardasani KR (2022) Simulation of disturbances in interdependent calcium and β -amyloid dynamics in the nerve cell. *Eur Phys J Plus* 137(8):1–23. <https://doi.org/10.1140/epjp/s13360-022-03164-x>
- Pawar A, Pardasani KR (2022) Study of disorders in regulatory spatiotemporal neurodynamics of calcium and nitric oxide. *Cognitive Neurodynamics* 1–22. <https://doi.org/10.1007/s11571-022-09902-2>
- Pawar A, Pardasani KR (2022) Effect of disturbances in neuronal calcium and IP_3 dynamics on β -amyloid production and degradation. *Cognitive Neurodynamics* 1–18. <https://doi.org/10.1007/s11571-022-09815-0>
- Pawar A, Raj Pardasani K (2022) Effects of disorders in interdependent calcium and IP_3 dynamics on nitric oxide production in a neuron cell. *Eur Phys J Plus* 137(5):1–19. <https://doi.org/10.1140/epjp/s13360-022-02743-2>
- Pawar A, Pardasani KR (2023) Computational model of calcium dynamics-dependent dopamine regulation and dysregulation in a dopaminergic neuron cell. *Eur Phys J Plus* 138(1):1–19
- Pathak KB, Adlakha N (2015) Finite element model to study calcium signalling in cardiac myocytes involving pump, leak and excess buffer. *J Med Imaging Health Inform* 5(4):683–688. <https://doi.org/10.1166/jmihi.2015.1443>

- Pathak K, Adlakha N (2016) Finite element model to study two dimensional unsteady state calcium distribution in cardiac myocytes. *Alexandria J Med* 52(3):261–268. <https://doi.org/10.1016/j.ajme.2015.09.007>
- Pedersen MG, Bertram R, Sherman A (2005) Intra- and inter-islet synchronization of metabolically driven insulin secretion. *Biophysical J* 89(1):107–119. <https://doi.org/10.1529/biophysj.104.055681>
- Pertusa JA, Sanchez-Andres JV, Martin F, Soria B (1999) Effects of calcium buffering on glucose-induced insulin release in mouse pancreatic islets: an approximation to the calcium sensor. *J Physiol* 520(Pt 2):473. <https://doi.org/10.1111/j.1469-7793.1999.00473.x>
- Rinzel J, Lee YS (1987) Dissection of a model for neuronal parabolic bursting. *J Math Biol* 25(6):653–75. <https://doi.org/10.1007/bf00275501> 358, 358
- Rorsman P (2005) Insulin secretion: function and therapy of pancreatic beta-cells in diabetes. *Br J Diabetes & Vasc Dis* 5(4):187–191. <https://doi.org/10.1177/147465140500500402>
- Rorsman P, Braun M, Zhang Q (2012) Regulation of calcium in pancreatic α - and β -cells in health and disease. *Cell Calcium* 51(3–4):300–308. <https://doi.org/10.1016/j.ceca.2011.11.006>
- Rorsman P, Braun M (2013) Regulation of insulin secretion in human pancreatic islets. *Annu Rev Physiol* 75:155–179. <https://doi.org/10.1146/annurev-physiol-030212-183754>
- Sabatini PV, Speckmann T, Lynn FC (2019) Friend and foe: β -cell Ca^{2+} signaling and the development of diabetes. *Mol Metab* 21:1–12. <https://doi.org/10.1016/j.molmet.2018.12.007>
- Singh N, Adlakha N (2019) A mathematical model for interdependent calcium and inositol 1, 4, 5-trisphosphate in cardiac myocyte. *Network Modeling Analysis in Health Informatics and Bioinformatics* 8(1):1–15. <https://doi.org/10.1007/s13721-019-0198-0>
- Singh N, Adlakha N (2019) Nonlinear dynamic modeling of 2-dimensional interdependent calcium and inositol 1, 4, 5-trisphosphate in cardiac myocyte. *Matematicheskaya Biologiya i Bioinformatika* 14(1), 290–305. <https://doi.org/10.17537/2019.14.290>
- Smith GD (1996) Analytical steady-state solution to the rapid buffering approximation near an open Ca^{2+} channel. *Biophysical J* 71(6):3064–3072. [https://doi.org/10.1016/S0006-3495\(96\)79500-0](https://doi.org/10.1016/S0006-3495(96)79500-0)
- Smith GD, Wagner J, Keizer J (1996) Validity of the rapid buffering approximation near a point source of calcium ions. *Biophysical J* 70(6):2527–2539. [https://doi.org/10.1016/S0006-3495\(96\)79824-7](https://doi.org/10.1016/S0006-3495(96)79824-7)
- Sneyd JAMES, Wetton BT, Charles AC, Sanderson MJ (1995) Intercellular calcium waves mediated by diffusion of inositol trisphosphate: a two-dimensional model. *Am J Physiol Cell Physiol* 268(6):C1537–C1545. <https://doi.org/10.1152/ajpcell.1995.268.6.C1537>
- Sneyd J, Falcke M (2005) Models of the inositol trisphosphate receptor. *Progress in biophysics and molecular biology* 89(3):207–245. <https://doi.org/10.1016/j.pbiomolbio.2004.11.001>
- Sprietsma JE, Schuitemaker GE (1994) Diabetes can be prevented by reducing insulin production. *Medical hypotheses* 42(1):15–23. [https://doi.org/10.1016/0306-9877\(94\)90029-9](https://doi.org/10.1016/0306-9877(94)90029-9)
- Tewari S, Pardasani KR (2010) Finite element model to study two dimensional unsteady state cytosolic calcium diffusion in presence of excess buffers. *IAENG Int J Appl Math* 40(3):108–112
- Tewari V, Tewari S, Pardasani KR (2011) A Model to Study the Effect of Excess buffers and Na^{+} ions on Ca^{2+} diffusion in Neuron cell. *Int J Bioeng Life Sci* 5(4):251–256
- Tewari SG, Pardasani KR (2011) Finite element model to study two dimensional unsteady state cytosolic calcium diffusion. *J Appl Math Inform* 29(1–2):427–442
- Tripathi A, Adlakha N (2013) Finite element model to study calcium diffusion in a neuron cell involving J_{RyR}, J_{SerCa} and J_{Leak}. *J Appl Math Inform* 31(5–6):695–709. <https://doi.org/10.14317/jami.2013.695>
- Varadi A, Molnr E, Ashcroft SJ (1995) Characterisation of endoplasmic reticulum and plasma membrane Ca^{2+} -ATPases in pancreatic β -cells and in islets of Langerhans. *Biochimica et Biophysica Acta (BBA)-Biomembranes* 1236(1):119–127. [https://doi.org/10.1016/0005-2736\(95\)00103-A](https://doi.org/10.1016/0005-2736(95)00103-A)
- Wagner J, Fall CP, Hong F, Sims CE, Allbritton NL, Fontanilla RA, Nuclli R (2004) A wave of IP_3 production accompanies the fertilization Ca^{2+} wave in the egg of the frog, *Xenopus laevis*: theoretical and experimental support. *Cell Calcium* 35(5):433–447. <https://doi.org/10.1016/j.ceca.2003.10.009>
- Wang M, Li J, Lim GE, Johnson JD (2013) Is dynamic autocrine insulin signaling possible? A mathematical model predicts picomolar concentrations of extracellular monomeric insulin within human pancreatic islets. *PLoS One* 8(6):e64860. <https://doi.org/10.1371/journal.pone.0064860>
- Li YX, Rinzel J (1994) Equations for InsP₃ receptor-mediated $[Ca^{2+}]_i$ oscillations derived from a detailed kinetic model: a Hodgkin-Huxley like formalism. *Journal of theoretical Biology* 166(4):461–473. <https://doi.org/10.1006/jtbi.1994.1041>

Publisher's Note Springer Nature remains neutral with regard to jurisdictional claims in published maps and institutional affiliations.

Springer Nature or its licensor (e.g. a society or other partner) holds exclusive rights to this article under a publishing agreement with the author(s) or other rightsholder(s); author self-archiving of the accepted manuscript version of this article is solely governed by the terms of such publishing agreement and applicable law.